JOURNAL OF THERMOPHYSICS AND HEAT TRANSFER
Vol. 23, No. 1, January–March 2009

Thermal Performance of an Axially Microgrooved Heat Pipe Using Carbon Nanotube Suspensions

Zhen-Hua Liu* and Lin Lu†
Shanghai Jiaotong University, Shanghai 200240, People's Republic of China

DOI: 10.2514/1.38190

An experimental investigation was carried out to study the heat transfer performance of an axially microgrooved heat pipe using water-based carbon nanotube suspensions as the working fluid. Experiments were performed under three steady operating pressures of 7.45, 12.38, and 19.97 kPa, respectively. Effects of the carbon nanotube mass concentration and the operating pressure on the evaporation and condensation heat transfer coefficients, the maximum heat flux, and the total heat resistance of the heat pipe were investigated and discussed. Experimental results show that carbon nanotube suspensions can apparently improve the thermal performance of the heat pipe and there is an optimal carbon nanotube mass concentration (about 2.0%) to achieve the maximum heat transfer enhancement. The operating pressure has a significant influence on the enhancement of heat transfer coefficients and slight influences on the enhancement of the maximum heat flux. Under the pressure of 7.45 kPa, the evaporation heat transfer coefficient and the maximum heat flux for the carbon nanotube suspension can be enhanced, at most, by about 80 and 25%, respectively, compared with those for water.

Nomenclature

h	=	heat transfer coefficient
L	=	heated length of the evaporator section
p	=	pressure
Q	=	heat input
q	=	heat flux
$q_{\max}$	=	maximum heat flux
R	=	heat resistance
r_0	=	outer radius of the evaporator of heat pipe
T	=	average temperature
T_i	=	inner wall temperature
T_s	=	saturation temperature of the steam
T_0	=	outer wall temperature
t_w	=	wall temperature
ΔT	=	wall superheat
λ	=	thermal conductivity
ω	=	mass concentration of carbon nanotube in suspension

Subscripts

c	=	condenser
CNT	=	carbon nanotube suspensions
e	=	evaporator
w	=	wall
0	=	water

I. Introduction

THE miniature or micro heat pipe has been applied as a reliable and efficient device for many years to cool microelectronic devices such as the CPUs of notebook computers. Generally, it is composed of an evaporator section, an adiabatic section, and a condenser section. In the development history of the heat pipe, many types (such as the thermosyphon, pulsating heat pipe, capillary pumped loop, loop heat pipe, grooved heat pipe, and micro heat pipe) have emerged, owing to the wisdom of their designers. The heat pipe with microgrooves is one of them. Without the need of external power, it is self-pumping due to the capillary force generated at the liquid–vapor interface. A large number of analytical studies [1–7] and experimental investigations have been devoted to heat transfer in microgrooved heat pipes [8–12].

Because the heat pipe uses the phase change of the working fluid to transfer heat, the selection of a working fluid is essential to achieve the maximum heat transfer. The nanofluid (nanoparticle suspension) was first applied by Choi [13] in thermal engineering due to its anomalous heat transfer characteristics. The nanofluid is a colloidal suspension with nanoparticles dispersed uniformly in a base fluid and has many unique characteristics in thermal engineering fields. Much research has been carried out to understand the thermophysical properties, natural/forced convective flow, and boiling heat transfer of nanofluids as well. Inspired by the enhanced heat transfer owing to nanofluids, some researchers, including the authors, have applied nanofluids in heat pipes to enhance the heat transfer performance. However, the little data can only draw a dim picture to understand heat transfer behaviors of nanofluids [14–20].

Particles in most nanofluids are pure metallic nanoparticles or metallic oxide nanoparticles. Carbon nanotube (CNT) is a new type of nanoscale material with a very high effective thermal conductivity. Therefore, the suspensions consisting of the CNT may have a better heat transfer performance than those consisting of the aforementioned particles. Based on this consideration, the present study used water-based CNT suspensions as the working liquid. The motivation of this paper was to provide a fundamental understanding of the application of water-based CNT suspensions in an axially microgrooved heat pipe. The effects of CNT suspensions on the evaporation and condensation heat transfer, the maximum heat flux, and the total heat resistance of the heat pipe were investigated. The study focused mainly on the heat transfer performance of the evaporator section, because the dominant heat resistance in a miniature heat pipe was on the evaporator section. A better heat transfer performance in the evaporator was found by substituting the CNT suspension for the deionized water. The experimental results are useful for designing miniature grooved heat pipes using the CNT suspension.

II. Experimental Apparatus and Procedure

In the present study, the CNT suspension consisting of deionized water and multiwall carbon nanotubes was used as the working liquid. The average diameter of carbon nanotubes was 15 nm and the

Received 23 April 2008; revision received 26 October 2008; accepted for publication 3 November 2008. Copyright © 2008 by the American Institute of Aeronautics and Astronautics, Inc. All rights reserved. Copies of this paper may be made for personal or internal use, on condition that the copier pay the $10.00 per-copy fee to the Copyright Clearance Center, Inc., 222 Rosewood Drive, Danvers, MA 01923; include the code 0887-8722/09 $10.00 in correspondence with the CCC.

*Professor, School of Mechanical Engineering; liuzhenh@sjtu.edu.cn (Corresponding Author).

†Doctor, School of Mechanical Engineering; lulin03@sjtu.edu.cn.

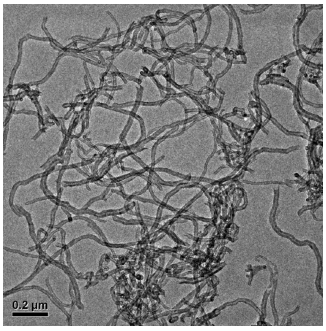

Fig. 1 TEM photograph of carbon nanotube suspension with a concentration of 1.0%.

length was in the range of 5–15 μm. The CNTs were first steeped in a mixture of sulphoacid and nitric acid for a few hours to break up their winding state. Then the CNTs were washed by pure water repeatedly until the pH value of the water reached 6.5. Finally, the suspension was oscillated continuously for 12 h in an ultrasonic water bath. Mass concentration of the CNT in the present experiment was in the range of 1.0 to 2.5 wt% and the corresponding volume concentration was 0.25 to 0.8%. A transmission electron microscope (TEM) photograph of the CNT suspension with a mass concentration of 1.0 wt% is shown in Fig. 1.

The experimental setup is shown schematically in Fig. 2. The heat pipe was a commercial product of Harbin Dawn Happy Heat Pipe Technology Co., Ltd., China. It was made of a copper tube with rectangular microgrooves fabricated in the inner wall. The heat pipe was positioned horizontally. The length, outer diameter, and wall thickness of the heat pipe were 350, 8, and 0.6 mm, respectively. The height and width of each rectangular groove were 0.2 and 0.25 mm, respectively, and the total number of grooves were 60. Lengths of the evaporator section, adiabatic section, and condenser section of the heat pipe were 100, 100, and 150 mm, respectively. The evaporator section was heated by an electrical heater, and the condenser section was cooled by water circulated in a constant-temperature water bath. The temperature and flow rate of the cooling water were accurately controlled to keep the operating pressure constant during each test.

Eight T-type thermocouples were welded on the outer wall surface of the test section. Four of them were at the evaporator section and three were at the condenser section. The other one was embedded into the adiabatic section to measure the steam temperature. Locations of the thermocouples are plotted in Fig. 3. A pressure transducer placed at the center of the adiabatic section measured the operating pressure of the heat pipe. The operating pressures were 7.45, 12.38, and 19.97 kPa, respectively, and the corresponding saturation temperatures were 40, 50, and 60°C, respectively. Experimental results show that the maximum difference between the measured saturation temperature and the calculated one based on the saturation pressure was only 0.2 K. Therefore, the measured steam temperature was used as the saturated steam temperature.

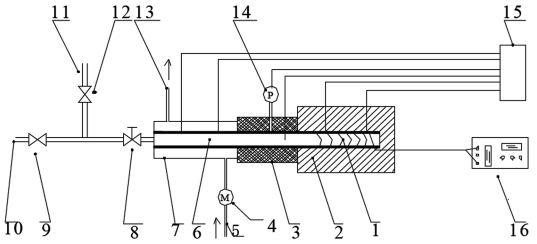

(1) Electrical heater. (2, 3) Insulation layers. (4) Flow meter. (5) Inlet of cooling water. (6) Test section. (7) Cooling jacket. (8, 9) Vacuum valve. (10) Liquid-filling inlet. (11) Vacuum-pumping inlet. (12) Vacuum valve. (13) Outlet of cooling water. (14) Pressure transducer. (15) Data acquisition system. (16) Rectifier.

Fig. 2 Schematic of the experimental apparatus.

During each test, the power was increasingly supplied to the electrical heater. A thermal cutout controller was installed in the power circuit to protect the experimental apparatus from excessive temperature. After each test ended, the heat pipe was left untouched for a week. Then the test was restarted and the experiment was repeated. No meaningful differences were found for the repeated tests. The reasons for the excellent repeatability should be that the thermal motion of CNTs caused the solution to be uniform again. For a uniformly dispersed solution, the repeating process could be easily guaranteed.

The CNT suspension was filled into the test section through a vacuum bullet valve. Before each test, a vacuum pumping process and a liquid preheating process were performed to remove the gases dissolved in the heat pipe and the working fluid. The minimum vacuum pressure during the pumping process was 0.086 Pa. The leakage rate of gases was about 0.8 Pa/h.

The liquid volume was fixed at half of the evaporator volume. According to the experimental result, this filling ratio was optimal for the maximum heat removal and minimum total heat resistance. In the present heat pipe, the groove volume was 1050 mm^3, the fill volume was 2358 mm^3, and the ratio of the groove volume to the liquid volume was about 0.45.

Figure 4 shows the diagram of the liquid charging and air pumping system. At the beginning of the experiment, the vacuum valves 16 and 17 were open during the vacuum pumping process. The vacuum pressure inside of the evaporator was measured by sensor 15. When the limit vacuum pressure was reached, the vacuum valve 17 was closed and the vacuum valve 18 was opened for the fluid-filling process.

The heat flux of the evaporator section q was calculated by

$$q = Q/(2\pi r_o L) \tag{1}$$

where Q is the heat input, r_o is the outer radius of the tube, and L is the heated length of the evaporator section. The inner wall temperature T_i is calculated by

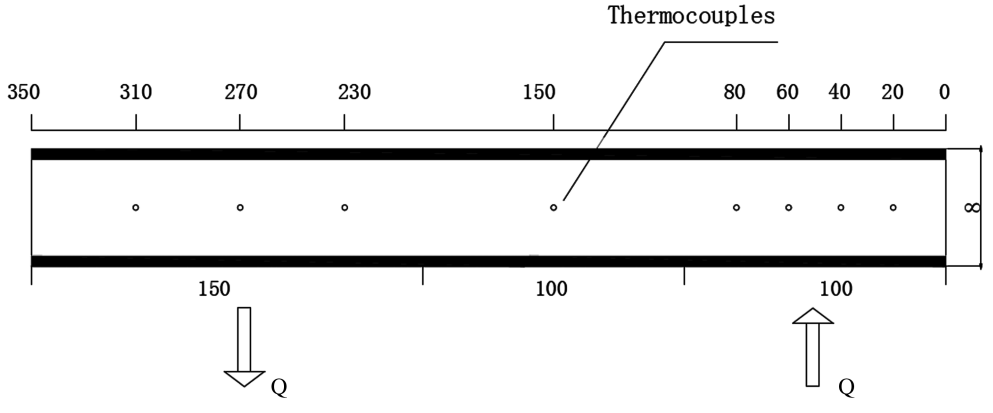

Fig. 3 Schematic of the test section (in millimeters).

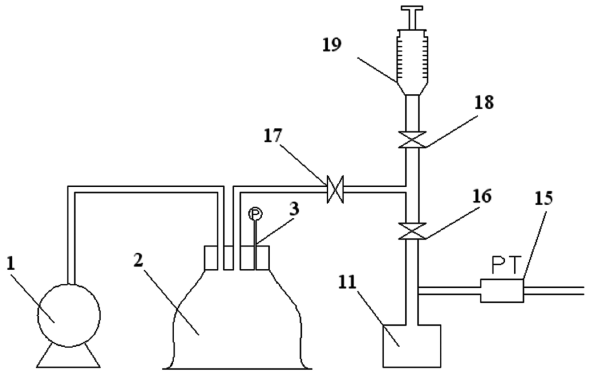

(1) Vacuum pump. (2) Glass container. (3) Pressure gauge. (11) Evaporator chamber. (15) Pressure transducer. (16, 17, 18) Vacuum valve. (19) Injector.

Fig. 4 Diagram of the liquid charging and vacuum pumping system.

$$T_i = T_o - \frac{qr_o}{\lambda_w} \ell n \frac{r_i}{r_o} \tag{2}$$

where T_o is the outer wall temperature of the heat pipe, λ_w is the thermal conductivity of copper, and r_i is the inner radius of the tube. In addition, wall superheat ΔT is calculated by the difference between the inner wall temperature T_i and the steam saturation temperature T_s. The heat transfer coefficient h is the ratio of the wall heat flux q to the wall superheat ΔT.

The energy balance between the evaporator and condenser was monitored in the study. The heat removed by the condenser was calculated from the volume flow rate and temperature increase of the cooling water. The energy balance was well observed, because the heat removed by the cooling water was greater than 96% of the input power.

In each test, the heating power was gradually increased by an increment of 5%. If the measured wall temperature increased abruptly and could not maintain a steady state, a dry-out phenomenon occurred on the wall. Simultaneously, the electric power supply was instantly switched off. Then the test was restarted at the previous steady state and the power was increased by an increment of 1%. When the dry-out phenomenon occurred again, the electric power supply was instantly switched off and the test was stopped. The maximum heat flux was determined.

The uncertainty of the measured temperature was 0.2 K. The maximum uncertainty of the pressure was 0.5%. The maximum uncertainties of the heat flux and heat transfer coefficient were 4 and 12%, respectively.

III. Results and Discussions

A. Wall Temperature Distributions for Deionized Water and the CNT Suspension

Figure 5 shows comparisons of the outer wall temperature distributions of the heat pipe using either deionized water or a CNT suspension with a 2% mass concentration. The operation pressure is 7.45 kPa. The wall temperature decreases along the test section for both fluids. In addition, the evaporation temperature increases and the condensation temperature decreases with the increase of of the heat input. At low heat inputs, wall temperature distributions are nearly the same for the CNT suspension and water. However, the evaporation temperature for the CNT suspension is lower than that for the deionized water at high heat inputs. The decrease of the evaporation temperature shows an apparent enhancement of evaporation heat transfer. The condensation temperature distributions for the CNT suspension are only slightly higher than those for the deionized water.

B. CNT Mass Concentration Effect on Evaporation and Condensation Heat Transfer Coefficients

Figure 6 shows the relation between the heat transfer coefficient and the heat flux of the evaporator. The mass concentration of CNTs

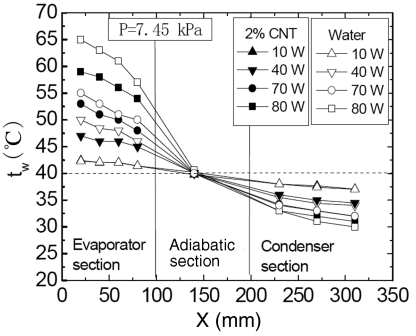

Fig. 5 Comparison between outer wall temperatures for water and CNT suspension at $p = 7.45$ kPa.

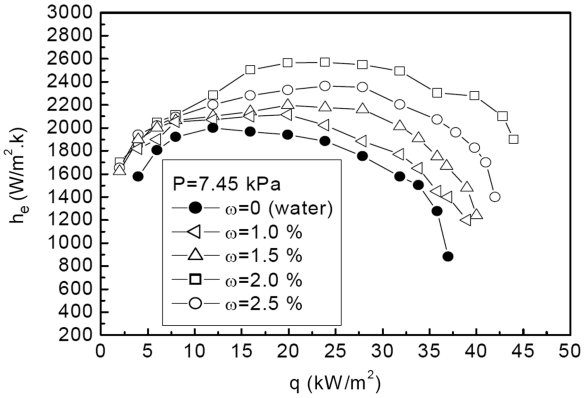

Fig. 6 Effect of mass concentration of nanoparticle on the evaporation heat transfer coefficient at $p = 7.45$ kPa.

is varied as a parameter. The operating pressure is 7.45 kPa. As shown in Fig. 6, the evaporation heat transfer coefficients of working liquids increase gradually at low heat fluxes. Then the heat transfer coefficients become saturated at moderate heat fluxes and finally decrease gradually at high heat fluxes. According to the relation between the heat transfer coefficient and the heat flux, it can be confirmed that the mechanisms of heat transfer in the evaporator are the convective evaporation heat transfer in the liquid-film layer in this study. At low heat fluxes, the natural convection may dominate the heat transfer and then the heat transfer coefficient increases with the increase of the heat flux. At moderate heat fluxes, the forced convection should govern the heat transfer and the heat transfer coefficient becomes nearly constant. However, at high heat fluxes, the local dry-out may occur, and the heat transfer coefficient decreases gradually as a consequence.

On the other hand, the evaporation heat transfer coefficients obviously increase with the increase of the CNT mass concentration from 0 to 2%. After that, the trend is weakened. It is clear that there exists an optimal CNT mass concentration for the maximum heat transfer enhancement. The optimal mass concentration is 2.0% for all test pressures.

Figure 7 shows the relation between the heat transfer coefficient and the heat flux of the condenser. The mass concentration of CNTs is varied as a parameter. The operating pressure is 7.45 kPa. As shown in Fig. 7, the condensation heat transfer enhancement of CNT suspensions is not obvious in the tested heat flux region, compared with that of water. Only an average enhancement of 10% can be obtained for the 2% CNT mass concentration suspension.

Figure 8 shows the relation between the ratio of effective thermal conductivities of CNT suspensions to that of water, λ_{CNT}/λ_0, liquid temperatures, and CNT mass concentrations. It is clear that the effective thermal conductivity of the CNT suspension with a 2% mass concentration increases by 20 to 25%, with regard to that of water in the tested temperature range. Therefore, the sole increase of effective thermal conductivity cannot cause a great increase in the heat transfer.

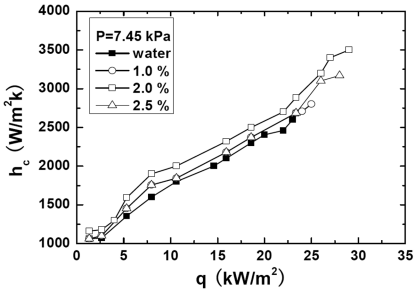

Fig. 7 Effect of mass concentration of nanoparticle on the condenser heat transfer coefficient at $P = 7.45$ kPa.

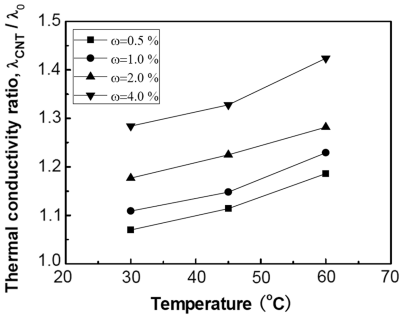

Fig. 8 Measured ratio of effective thermal conductivity of CNT suspensions to that of water.

In the present study, the convective evaporation and condensation heat transfer in the liquid film dominate the thermal performance of the grooved heat pipe. The heat transfer enhancement of CNT suspensions in the heat pipe may result for four reasons. First, the increase of the effective thermal conductivity of the CNT suspension can enhance the conductive heat transfer. Second, the increase of the effective density of the CNT suspension can enhance the forced convective heat transfer. Third, the decease of the solid–liquid contact angle between the CNT suspension and the wall can increase the capillary force. These three reasons all result from the different thermophysical properties of CNT suspensions. The fourth is attributed to the turbulence effect of random motion (Brownian motion) of CNTs in the base liquid, and it is a nanoscale effect.

To demonstrate the random motion of CNTs, a mixture of water and CNTs was poured into a Bunsen beaker and then the bottom of the Bunsen beaker was heated. It was clearly observed that CNTs moved violently in water. This random motion results from the liquid buoyant force and Brownian motion of CNTs, and it is called the turbulence effect of CNT suspensions.

In the evaporator section, only a little amount of CNTs can pass through the gas–liquid interface and are carried by steam to the condenser section. Only a little amount of CNTs exist in the liquid film in the condenser section. Therefore, the enhancement of the condensation heat transfer is weak.

In the present experiment, tests were carried out with the increase of the heat flux. At the beginning of the tests, most CNTs deposit on the bottom of the suspension and the turbulence effect of CNTs is weak; hence, the heat transfer enhancement is weak at low heat fluxes. With the increase of the heat flux, the deposited CNTs can quickly spread into the base liquid, forming a uniform suspension again. Therefore, the heat transfer enhancement effect gradually increases with the increase of the heat flux.

C. Operating Pressure Effect on the Enhancement Ratio of Evaporation Heat Transfer Coefficient

Figure 9 shows the dependence of the enhancement ratio of evaporation heat transfer coefficient, which is defined as the ratio of the evaporation heat transfer coefficient of the CNT suspension with a 2% CNT mass concentration to that of water. The operating pressure is varied as a parameter. At low heat fluxes, the ratio is

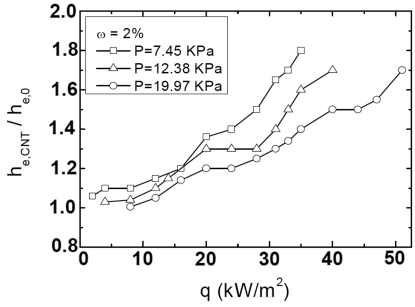

Fig. 9 Effect of operating pressure on the evaporation heat-transfer-coefficient enhancement.

basically close to unity and there is no meaningful heat transfer enhancement. Then with the increase of heat fluxes, the enhancement ratio increases gradually for all test pressures. Note that the enhancement ratio increases with the decrease of operating pressures. For the pressure of 7.45 kPa, the maximum and the average enhancement ratios can reach about 1.8 and 1.4, respectively.

Note that the enhancement ratio increases with the decrease of operating pressures. At the pressure of 7.45 kPa, the maximum and the average enhancement ratios can reach about 1.8 and 1.4, respectively. However, at the pressure of 19.97 kPa, the maximum and the average enhancement ratio reach about 1.7 and 1.25, respectively. The reason cannot be well explained in the current stage.

D. Operating Pressure Effect on the Enhancement Ratio of the Maximum Heat Flux

Figure 10 shows the effect of the mass concentration on the enhancement ratio of the maximum heat flux, which is defined as the ratio of the maximum heat flux for suspensions to that for deionized water, with the operating pressure as a parameter. All ratios increase with the increase of the mass concentration at the beginning and decrease thereafter. The mass concentration of 2.0% corresponds to the maximum ratio of the maximum heat flux for all pressures, which is in accordance with the results obtained for the maximum heat-transfer-coefficient ratio. At the mass concentration of 2.0%, the maximum heat flux is increased by about 20, 18, and 25%, respectively, under the pressures of 19.97, 12.38, and 7.45 kPa. If considering some test uncertainties, it may be concluded that the enhancement ratio of the maximum heat flux slightly increases with the decrease of the operating pressure.

The maximum heat flux enhancement may result for two reasons: the formation of a thin porous coating layer on the inner wall surface and the decease of the solid–liquid contact angle between the wall and the CNT suspension. They all lead to an increase of the capillary force and enhancement of the maximum heat flux.

The presence of a thin porous layer on the wall was confirmed by the present experimental observation. A TEM photograph of the porous layer was attempted and failed, because the regular tube had grooves that could not be smoothed out. The thin porous layer should

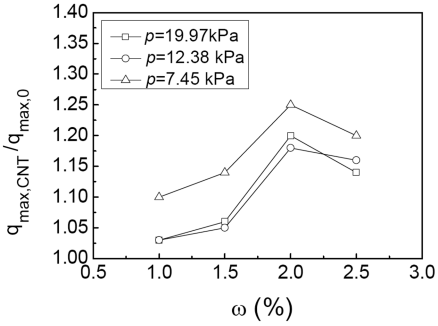

Fig. 10 Effect of operating pressure on the maximum heat flux enhancement.

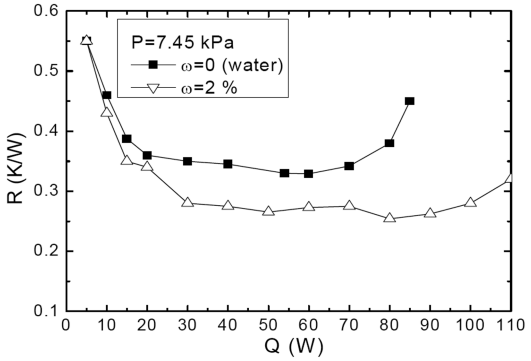

Fig. 11 Comparison between total heat resistances for water and CNT suspension at $P = 7.47$ kPa.

consist of the chips of CNTs inlaid in the very small surface slots on the wall surface. This CNT thin layer cannot be cleaned out completely by a water, jet but it can be cleaned out completely by a weak acid liquid. This porous layer can provide a pumping effect to pull the liquid to the wall. Liquid with this layer can be more sufficiently supplied. Also, the existence of the porous layer can also reduce the solid–liquid contact angle, which leads also to an increase of the capillary force and enhancement of the maximum heat flux.

E. CNT Suspension Effect on the Total Heat Resistance of the Heat Pipe

Figure 11 displays the effect of the suspension with a 2% CNT mass concentration on the total heat resistance of the heat pipe at the pressure of 7.45 kPa. The total heat resistance is defined as

$$R = (\bar{T}_e - \bar{T}_c)/Q \tag{3}$$

where $\bar{T}_e$ and $\bar{T}_c$ are the average temperatures of the evaporator and condenser sections, respectively.

At low heat inputs, the total heat resistances are basically the same for the suspension and water. With the increase of the heat inputs, the total heat resistance for the suspension decreases reasonably, compared with that for water. When the heat flux is over 70 $\mathrm{kW/m^2}$, the total heat resistance of the heat pipe using deionized water increases sharply, indicating the occurrence of dry-out. When the heat flux is over 85 $\mathrm{kW/m^2}$, the heat pipe using deionized water fails. However, the heat pipe using the CNT suspension can still work well and has a lower total heat resistance. In the range $q < 85$ $\mathrm{kW/m^2}$, the total heat resistance of the heat pipe using the CNT suspension can be decreased, on average, by about 20%, compared with that using water, at the pressure of 7.45 kPa.

The total heat resistance of the heat pipe consists of the evaporation and condensation heat resistances. In general, the condensation heat resistance can be easily decreased with the increase of the heat transfer surface area of the condenser in electronic devices; hence, decreasing evaporation heat resistance is a key issue for enhancing thermal performance of heat pipes.

To sum up, it is confirmed that CNT suspensions with a mass concentration of 2.0% as the working fluid can evidently strengthen the evaporation heat transfer coefficient and the maximum power input under subatmospheric pressures. The CNT suspension has the potential and applicable prospect of enhancing the thermal performance of grooved heat pipes.

IV. Conclusions

1) Wall temperatures of the microgrooved heat pipe using CNT suspensions are lower than those using deionized water at moderate and high heat inputs. The temperature distributions tend to be more uniform for the heat pipe using CNT suspensions.

2) The heat flux has a significant effect on the heat transfer enhancement of CNT suspensions. At low heat fluxes, CNT suspensions have no meaningful effects on the heat transfer enhancement. With the increase of heat fluxes, the enhancement of CNT suspensions on the heat transfer becomes stronger.

3) At moderate and high heat fluxes, the heat transfer coefficient of the evaporator section increases with mass concentration when the mass concentration is less than 2.0%. Then they decrease when the mass concentration is larger than 2.0%. The mass concentration of 2.0% corresponds to the optimal heat transfer enhancement. The heat transfer coefficient of the evaporator section can be enhanced, at most, by about 80% and the maximum heat flux can be enhanced, at most, by about 25% if the 2.0% CNT suspension is used instead of the deionized water.

4) The operating pressure has an apparent influence on the enhancement of the heat transfer coefficient and a slight influence on the enhancement of the maximum heat flux. Both enhancements increase with the decrease of the operating pressure.

5) The total heat resistance of the heat pipe obviously decreases, and the maximum power of the heat pipe evidently increases when the deionized water is substituted by the 2.0% CNT suspension.

Acknowledgment

This study was supported by the Key Foundational Research Project of Science and Technology Bureau of Shanghai under grant no. 04JC14049.

References

[1] Cotter, T. P., "Principles and Prospects of Micro Heat Pipes," *Proceedings of the 5th International Heat Pipe Conference*, Japan Association for Heat Pipes, Tsukuba, Japan, 1984, pp. 328–335.

[2] Peterson, G. P., and Ma, H. B., "Theoretical Analysis of the Maximum Heat Transport in Triangular Grooves: A Study of Idealized Micro Heat Pipe," *Journal of Heat Transfer*, Vol. 118, No. 3, 1996, pp. 731–739. doi:10.1115/1.2822693

[3] Suman, B., and Hoda, N., "Effect of Variations In Thermophysical Properties and Design Parameters on the Performance of a *V*-Shaped Micro Grooved Heat Pipe," *International Journal of Heat and Mass Transfer*, Vol. 48, No. 10, 2005, pp. 2090–2101. doi:10.1016/j.ijheatmasstransfer.2005.01.007

[4] Wu, D., and Peterson, G. P., "Investigation of the Transient Characteristics of a Micro Heat Pipe," *Journal of Thermophysics and Heat Transfer*, Vol. 5, No. 2, 1991, pp. 129–134. doi:10.2514/3.239

[5] Suman, B., De, S., and DasGupta, S., "Transient Modeling of Micro-Grooved Heat Pipe," *International Journal of Heat and Mass Transfer*, Vol. 48, No. 8, 2005, pp. 1633–1646. doi:10.1016/j.ijheatmasstransfer.2004.11.004

[6] Jiao, A. J., Ma, H. B., and Critser, J. K., "Evaporation Heat Transfer Characteristics of a Grooved Heat Pipe with Micro-Trapezoidal Grooves," *International Journal of Heat and Mass Transfer*, Vol. 50, Nos. 15–16, 2007, pp. 2905–2911. doi:10.1016/j.ijheatmasstransfer.2007.01.009

[7] Lin, L. C., and Faghri, A., "Heat Transfer in Micro Region of a Rotating Miniature Heat Pipe," *International Journal of Heat and Mass Transfer*, Vol. 42, No. 8, Apr. 1999, pp. 1363–1369. doi:10.1016/S0017-9310(98)00270-1

[8] Hopkins, R., Faghri, A., and Khrustalev, D., "Flat Miniature Heat Pipes with Micro Capillary Grooves," *Journal of Heat Transfer*, Vol. 121, No. 1, 1999, pp. 102–109. doi:10.1115/1.2825922

[9] Kim, S. J., Seo, J. K., and Do, K. H., "Analytical and Experimental Investigation on the Operational Characteristics and the Thermal Optimization of a Miniature Heat Pipe with a Grooved Wick Structure," *International Journal of Heat and Mass Transfer*, Vol. 46, No. 11, 2003, pp. 2051–2063. doi:10.1016/S0017-9310(02)00504-5

[10] Kang, S. W., Tsai, S. H., and Chen, H. C., "Fabrication and Test of Radial Grooved Micro Heat Pipes," *Applied Thermal Engineering*, Vol. 22, No. 14, 2002, pp. 1559–1568. doi:10.1016/S1359-4311(02)00085-6

[11] Chien, H. T., Lee, D. S., Ding, P. P., Chiu, S. L., and Chen, P. H., "Disk-Shaped Miniature Heat Pipe (DMHP) with Radiating Micro Grooves for a To can Laser Diode Package," *IEEE Transactions on Components and Packaging Technologies*, Vol. 26, No. 3, 2003, pp. 569–574. doi:10.1109/TCAPT.2003.817648

[12] Kang, S. W., and Huang, D. L., "Fabrication of Star Grooves and Rhombus Grooves Micro Heat Pipe," *Journal of Micromechanics and Microengineering*, Vol. 12, No. 5, 2002, pp. 525–531. doi:10.1088/0960-1317/12/5/303

[13] Choi, S. U. S., "Enhancing Thermal Conductivity of Fluids with Nanoparticles, *Development and Applications of Non-Newtonian Flows*, Vol. 231, edited by D. A. Siginer and H. P. Wang, American Society of Mechanical Engineers, New York, 1995, pp. 99–105.

[14] Tsai, C. Y., Chien, H. T., Ding, P. P., Chan, B., Luh, T. Y., and Chen, P. H., "Effect of Structural Character of Gold Nano-Particles in Nanofluid on Heat Pipe Thermal Performance," *Materials Letters*, Vol. 58, No. 9, 2004, pp. 1461–1465. doi:10.1016/j.matlet.2003.10.009

[15] Wei, W. C., Tsai, S. H., Yang, S. Y., and Kang, S. W., "Effect of Nanofluid Concentration on Heat Pipe Thermal Performance," *IASME Transactions*, Vol. 2, No. 8, 2005, pp. 1432–1439.

[16] Kang, S. W., Wei, W. C., Tsai, S. H., and Yang, S. Y., "Experimental Investigation of Silver Nano-Fluid on Heat Pipe Thermal Performance," *Applied Thermal Engineering*, Vol. 26, Nos. 17–18, 2006, pp. 2377–2382. doi:10.1016/j.applthermaleng.2006.02.020

[17] Ma, H. B., Wilson, C., Borgmeyer, B., Park, K., Yu, Q., Choi, S. U. S., and Tirumala, M., "Effect of Nanofluid on the Heat Transport Capability in an Oscillating Heat Pipe," *Applied Physics Letters*, Vol. 88, No. 14, 2006, pp. 143116.1–143116.3.

[18] Xue, H. S., Fan, J. R., Hu, Y. C., Hong, R. H., and Cen, K. F., "The Interface Effect of Carbon Nanotube Suspension on the Thermal Performance of a Two-Phase Closed Thermosyphon," *Journal of Applied Physics*, Vol. 100, No. 10, 2006, pp. 104909.1–104909.5.

[19] Liu, Z. H., Yang, X. F., and Guo, G. L., "Effect of Nanoparticles in Nanofluid on Thermal Performance in a Miniature Thermosyphon," *Journal of Applied Physics*, Vol. 102, No. 1, 2007, pp. 013526.1–013526.8.

[20] Liu, Z. H., Xiong, J. G., and Bao, R., "Boiling Heat Transfer Characteristics of Nanofluids in a Flat Heat Pipe Evaporator with Micro-Grooved Heating Surface," *International Journal of Multiphase Flow*, Vol. 33, No. 12, 2007, pp. 1284–1295. doi:10.1016/j.ijmultiphaseflow.2007.06.009